GENERALIZED KDV EQUATION: NOVEL NATURE OCEANIC, M-LUMP AND PHYSICAL COLLISION WAVES

Hajar Farhan ISMAEL*/**

*Department of Mathematics, College of Science, University of Zakho, Zakho, Iraq
**Department of Computer Science, College of Science, Knowledge University, Erbil 44001, Iraq

hajar.ismael@uoz.edu.krd

received 30 November 2024, revised 8 February 2025, accepted 10 February 2025

Abstract: The main idea of this study is to explore new features for the generalized (3+1)-dimensional Korteweg-De Vries problem. This equation may be used to model various physical processes in several domains, including nonlinear optics, oceanography, acoustic waves in plasma physics, and other areas where coupled wave dynamics are essential. The Hirota method and long-wave technique to reveal various wave solutions are under consideration. Complex N-soliton solutions, M-lump waves, and hybrid solutions between some types of soliton and M-lump solutions are offered. The obtained solutions are one-, two-, and three-M-lump waves and mixed soliton-lump, soliton-two-lump, and two-soliton-lump solutions. Also, one-soliton, two-soliton, three-soliton, and four-soliton solutions in complex form are offered. To better analyse and understand the propagation characteristics of these solutions, 3D and contour plots for gained solutions are drawn. As far as we know, these solutions are novel and have not been revealed. Since the KdV equation often describes shallow water waves with weakly nonlinear restoring forces, we are interested in the features that have yet to be studied.

Key words: complex multi-soliton, hybrid wave, Hirota bilinear method, long-wave method

1. INTRODUCTION

Nonlinearity is a fascinating phenomenon in nature, and scientists believe that nonlinear study is the most promising means of gaining a deeper understanding of how nature works. Investigating a wide range of nonlinear ordinary and partial differential equations is critical for mathematically describing complicated processes that change over time. These mathematical formulas are created in various fields, including economics, optical fibers, elasticity, plasma physics, solid-state physics, population ecology, infectious disease epidemiology, physics, and natural sciences. Soliton solutions of the previously mentioned phenomenon have been a fascinating and extraordinarily active topic of study for the past several decades, with the accompanying problem being the creation of exact solutions to a large variety of nonlinear partial differential equations. As a result, mathematics and physical scientists have made significant efforts to develop exact wave solutions to certain NLPDEs and various practical and potent strategies, including Hirota's method [1][2][3][4], Backlund transformations [5], Pfaffian technique [6], the extended simplest equation approach [7], Riemann–Hilbert method [8][9], modified Sardar sub-equation method [10], physics-informed neural networks algorithm [11], a unified method [12], bilinear Bäcklund transformation [13], modified F-expansion method [14], the symbolic computation and Hirota method [15], and so on.

A soliton is a single, self-reinforcing wave that passes over a medium without ever dispersing or dissipating, preserving its shape and speed. Solitons are extremely stable and may maintain their form over long distances due to their unique nature. A lump solution is an analytical rational function solution that exists in all directions in space, and solitons are analytic solutions that are exponentially localized in all directions in space and time. They have previously been identified for nonlinear integrable equations.

A well-known partial differential equation used to model the disturbance of the surface of shallow water in the presence of solitary waves is the Korteweg-De Vries (KdV) equation. This equation incorporates leading-order nonlinearity and dispersion and can be used to study weakly nonlinear long waves. In shallow water, it describes small-amplitude waves with long wavelengths. The KdV equations have different types, such as the fifth-order KdV equation [16], the lattice potential KdV equation [17], generalized geophysical KdV equation [18], modified KdV equation [19], seventh-order KdV equation [20], Schwarzian KdV equation [21], and many others.

Recently, the generalized Korteweg-De Vries (gKdV) equation in two dimensions became known and read as follows:

$$u_t + 6uu_x + u_{xxx} + u_x + \partial_x^{-1}u_{yt} + u_y + u_{xxy} + 3uu_y + 3u_x\partial_x^{-1}u_y = 0, \tag{1}$$

where $\partial_x^{-1} \cdot := \int_{-\infty}^{x} \cdot\, dx$. It is comparable to the following equation when accounting for the potential $u(x, y, z, t) = \theta(x, y, z, t)$

$$\theta_{xt} + 6\theta_x\theta_{xx} + \theta_{xxxx} + \theta_{xx} + \theta_{yt} + \theta_{xy} + \theta_{xxxy} + 3\theta_x\theta_{xy} + 3\theta_{xx}\theta_y = 0. \tag{2}$$

Lu and Chen [22] investigated this problem and found many distinct solutions in addition to integrability results. By modifying the preceding (2+1)-dimensional form (1), Ismaeel et al. [23], have created a new (3+1)-dimensional integrable gKdV equation.

$$u_t + 6uu_x + u_{xxx} + u_x + \partial_x^{-1}u_{yt} + u_y + u_{xxy} + 3uu_y + 3u_x\partial_x^{-1}u_y + \beta u_z + \beta_1\partial_x^{-1}u_{yz} + \gamma\partial_x^{-1}u_{yy} = 0, \tag{3}$$

DOI 10.2478/ama-2025-0026

where β, β_1, γ are defined as non-zero constants. The Painlev´e test to reveal the integrability of the equation was used and found that when $\beta = \beta_1$, the equation becomes integrable. Therefore, we have

$$u_t + 6uu_x + u_{xxx} + u_x + \partial_x^{-1}u_{yt} + u_y + u_{xxy} + 3uu_y + 3u_x\partial_x^{-1}u_y + \beta u_z + \beta\partial_x^{-1}u_{yz} + \gamma\partial_x^{-1}u_{yy} = 0. \quad (4)$$

The multiple soliton solutions to the equation (4) were reported by authors in Ref. [23]. In this paper, we use Hirota's method, which is a direct method to obtain multiple soliton solutions to integrable nonlinear evolution equations. It is also possible to determine multiple soliton solutions using other methods, such as inverse scattering transform [24] and various other techniques. The advantage of Hirota's method over the others is that it is algebraic rather than analytic. Therefore, Hirota's method provides the most efficient results when we just want to construct multiple soliton solutions. Also, applying the long-wave method on N-soliton solutions, we can offer M-lump waves. In the present study, one-, two-, and three-M-lump waves, three interaction phenomena of soliton with M-lump waves, and four types of complex multiple solutions are derived. To our knowledge, these propagation wave solutions have not been investigated before.

Following is a summary of this study: In the second section, under the corresponding N-soliton solutions, the main idea is to construct M-lump solutions for equation (4), which is made possible by using a long wave method. In the third section, we offer and analyze the characteristics of mixed solutions, a mix of lump and soliton solutions. The fourth section is about the complex N-soliton solutions for the studied equation. In the fifth section, results and discussion about constructed solutions are presented. The last part contains some discussions and conclusions from this effort.

2. MULTIPLE M-LUMP SOLUTIONS

To extract the soliton solutions to the Eq. (4), consider the relation

$$u = 2(log(f))_{xx}. \quad (5)$$

Therefore, equation (4) could be shown to possess its bilinear form

$$\begin{pmatrix} D_tD_x + D_yD_t + D_xD_y + D_x^4 + D_x^3D_y + \\ D_x^2 + \beta D_xD_z + \beta D_yD_z + \gamma D_y^2 \end{pmatrix} f.f = 0, \quad (6)$$

where $f = f(x, y, z, t)$ and D is the Hirota derivative and stated as

$$D_{x_1}^{r_1}D_{x_2}^{r_2}D_{x_3}^{r_3}D_{x_4}^{r_4}\chi_1.\chi_2 = \left(\partial_{x_1} - \partial_{x_1'}\right)^{r_2}\left(\partial_{x_2} - \partial_{x_2'}\right)^{r_4} \times \left(\partial_{x_3} - \partial_{x_3'}\right)^{r_3}\left(\partial_{x_4} - \partial_{x_4'}\right)^{r_4} \times \chi_1(x_1, x_2, x_3, x_4)\chi_2(x_1', x_2', x_3', x_4')|_{x_1=x_1', x_2=x_2', x_3=x_3', x_4=x_4'},$$

where x_1, x_2, x_3, x_4 defines as independent variables, χ_1, $\chi_2$are dependent variables, and constants $r_1, r_2, r_3, r_4 \geq 0$. Generally, to offer the N-soliton solutions to the PDEs, we use the following formula [25]:

$$f \equiv f_N = \sum_{\mu=0,1} exp\left(\sum_{m=1}^{N} \Omega_m\varphi_m + \sum_{m<n}^{(N)} \mu_m\mu_n A_{mn}\right) \quad (7)$$

The notation $\sum_{\mu=0,1}$ represents the sum of all possible composites $\mu_m = 0,1$, for $m = 1,2, \ldots, N$.

By taking the specific condition $m < n$, the first three solutions of Eq. (7) have the form

$$\begin{aligned} &f_1=1+e^{\Omega_1}, \\ &f_2 = 1 + e^{\Omega_1} + e^{\Omega_2} + A_{12}e^{\Omega_1+\Omega_2}, \\ &f_3 = 1 + e^{\Omega_1} + e^{\Omega_2} + e^{\Omega_3} + A_{12}e^{\Omega_1+\Omega_2} + A_{13}e^{\Omega_1+\Omega_3} + \\ &A_{23}e^{\Omega_2+\Omega_3} + A_{123}e^{\Omega_1+\Omega_2+\Omega_3}, \end{aligned} \quad (8)$$

where

$$\Omega_m = k_m(x + l_my + j_mz + w_mt) + \lambda_m, \quad (9)$$

with dispersion relation

$$w_m = -\left(1 + {k_m}^2 + j_m\beta + \frac{{l_m}^2\gamma}{1+l_m}\right), \quad (10)$$

and

$$e^{A_{mn}} = \frac{K_1}{K_2}, \quad (11)$$

where

$$\begin{aligned} &K_1 = 3(k_m - k_n)(1 + l_m)(1 + l_n)\big(k_m(1 + l_m) - k_n(1 + l_n)\big) - (l_m - l_n)^2\gamma, \\ &K_2 = 3(k_m + k_n)(1 + l_m)(1 + l_n)(k_m + k_n + k_ml_m + k_nl_n) - (l_m - l_n)^2\gamma. \end{aligned}$$

Here, $k_m, l_m, j_m, w_m, \lambda_m$ are constants, whereas Ω_m defines as the functions dependent on x, y, z, t. Now, to address the M-lump wave solution, we apply the long-wave method by taking $N = 2$, and assuming, $k_m \to 0$, $e^{\lambda_m} = -1$, and $\frac{k_1}{k_2} = O(1)$ in Eq. (7) give

$$f_2 = \Phi_1\Phi_2 + B_{12}, \quad (12)$$

where

$$\Phi_m = x + l_my + j_mz + w_mt, \quad (13)$$

$$w_m = -\left(1 + j_m\beta + \frac{{l_m}^2\gamma}{1+l_m}\right), \quad (14)$$

$$B_{mn} = \frac{6(1+l_m)(1+l_n)(2+l_m+l_n)}{(l_m-l_n)^2\gamma}. \quad (15)$$

Taking $l_1 = a_1 + b_1i$, $l_2 = l_1^*$ and $j_1 = c_1 + d_1i$, $j_2 = j_1^*$. Note that $i = \sqrt{-1}$ and $*$ indicates the complex conjugation. From plugging Eqs. (12-15) into Eq. (5), we have

$$u = 2\left(log\left(\begin{matrix}\left(x' + a_1y' + c_1z'\right)^2 + \left(b_1y' + d_1z'\right)^2 \\ -\frac{3(1+a_1)((1+a_1)^2+{b_1}^2)}{{b_1}^2\gamma}\end{matrix}\right)\right)_{xx} \quad (16)$$

where

$$\begin{aligned} &x' = \frac{\gamma\, a_1 + \gamma\, {b_1}^2 + \gamma\, {a_1}^2}{{a_1}^2+{b_1}^2+2a_1+1}t - t, \\ &y' = y - \gamma\, t, \\ &z' = z - \beta\, t. \end{aligned}$$

Equation (16) is a single M-lump wave as shown in Figure (1) for the gKdV equation with decaying as $O\left(\frac{1}{x^2}, \frac{1}{y^2}, \frac{1}{z^2}\right)$ for $|x|, |y|, |z| \to \infty$ and move with the velocity

$$\begin{aligned} &v_x = 1 - \frac{(a_1+{b_1}^2+{a_1}^2)\,\gamma}{({a_1}^2+{b_1}^2+2a_1+1)}, \\ &v_y = \gamma\,, \end{aligned}$$

$v_z = \beta$.

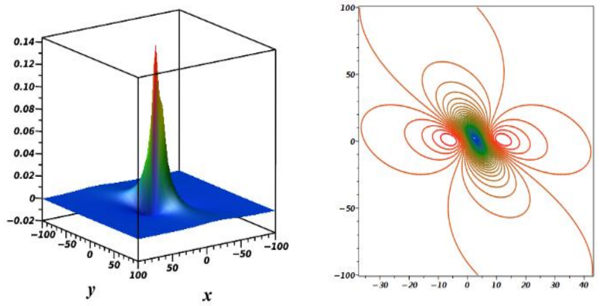

Fig. 1. Graphs of one-M-lump wave when $\boldsymbol{z = 2, t = 2, a_1 = \frac{1}{5}, b_1 = 0.5, c_1 = 0.5, d_1 = 0.5, \beta = 2, \gamma = -1}$.

The path followed by this wave is denoted by the following plane:

$y = \frac{G_1}{G_2}$,.

where

$$G_1 = -\left(\left((a_1+1)^2 + {b_1}^2\right)d_1(z - x\beta)\right) - \left({a_1}^2(1 + a_1) + (a_1 - 1){b_1}^2\right)d_1 z\gamma + b_1\left(a_1(a_1 + 2) + {b_1}^2\right)(x + c_1 z)\gamma,$$
$$G_2 = \left((a_1+1)^2 + {b_1}^2\right)(b_1 + b_1 c_1\beta - a_1 d_1\beta) - b_1\left({a_1}^2 + {b_1}^2\right)\gamma.$$

The one-M-lump wave on this plane is depicted in Figure (2) at various time periods.

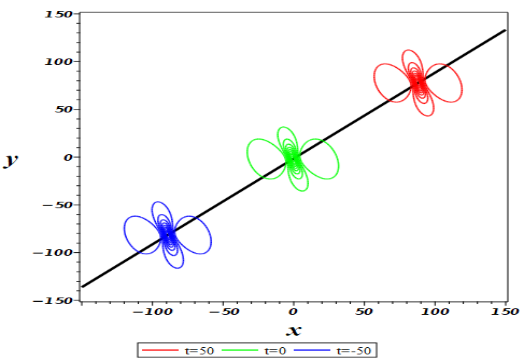

Fig. 2. Plot of Eq. (12) for $\boldsymbol{z = 2, a_1 = \frac{1}{5}, b_1 = 0.5, c_1 = 0.5, d_1 = 0.5, \beta = 2, \gamma = -1}$

As part of our analysis of the equation, we want to specify the characteristics of a double-M-lump wave by considering $N = 4$ in Eq. (7), and $k_m \to 0$, $e^{\lambda_m} = -1$ $(m = 1,2,3,4)$, the outcome offers

$$f_4 = \Phi_1\Phi_2\Phi_3\Phi_4 + B_{12}\Phi_3\Phi_4 + b_{13}\Phi_2\Phi_4 + B_{14}\Phi_2\Phi_3 + B_{23}\Phi_1\Phi_4 + B_{24}\Phi_1\Phi_3 + B_{34}\Phi_1\Phi_2 + B_{12}\Phi_{34} + B_{13}B_{24} + B_{14}B_{23}, \tag{17}$$

where $\Phi_1, \Phi_2, \Phi_3, \Phi_4, w_m$ and B_{mn} $(n < m)$ are explained with Eqs. (13), (14), and Eq. (15), respectively. The double-lump solution is obtained by combining equation (17) with the other findings in equation (5) and demonstrated in Figure 3.

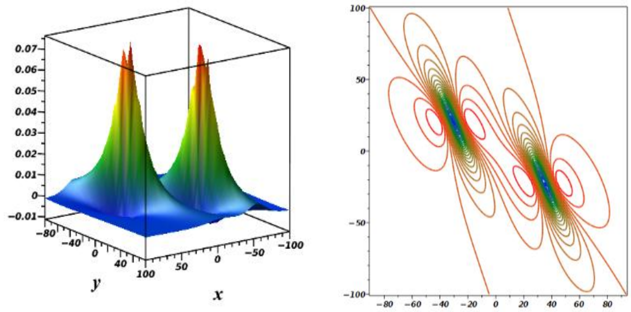

Fig. 3. Plots of 2-M-lump wave when $\boldsymbol{z = 2, t = 2, a_1 = 0.5, b_1 = 0.5, a_2 = \frac{1}{3}, b_2 = \frac{1}{3}, c_1 = \frac{1}{3}, d_1 = \frac{1}{3}, c_2 = \frac{1}{4}, d_2 = \frac{1}{4}, \beta = 2, \gamma = -1}$.

For 3-M-lump of Eq. (4), we take $k_m \to 0$, $e^{\lambda_m} = -1$ $(m = 1, \dots, 6)$ and considering $N = 6$ in Eq. (7), shows

$$\begin{aligned}
f_6 = {} & \Phi_1\Phi_2\Phi_3\Phi_4\Phi_5\Phi_6 + B_{12}B_{34}B_{56} + B_{12}B_{35}B_{46} + B_{12}B_{45}B_{36} + B_{13}B_{24}B_{56} + B_{13}B_{25}B_{46} + B_{13}B_{45}B_{26} + \\
& B_{23}B_{14}B_{56} + B_{14}B_{25}B_{36} + B_{14}B_{35}B_{26} + B_{24}B_{15}B_{36}B_{34}B_{15}B_{26} + B_{23}B_{15}B_{46} + B_{23}B_{45}B_{16} + \\
& B_{24}B_{35}B_{16} + B_{34}B_{25}B_{16} + \Phi_2\Phi_3\Phi_4\Phi_5B_{16} + \Phi_2\Phi_3\Phi_5\Phi_6B_{14} + \Phi_2\Phi_3\Phi_4\Phi_6B_{15} + \Phi_3\Phi_4\Phi_5\Phi_6B_{12} + \\
& \Phi_2\Phi_4\Phi_5\Phi_6B_{13} + \Phi_1\Phi_2\Phi_4\Phi_6B_{35} + \Phi_1\Phi_2\Phi_4\Phi_5B_{36} + \Phi_1\Phi_4\Phi_5\Phi_6B_{23} + \Phi_1\Phi_3\Phi_5\Phi_6B_{24} + \Phi_1\Phi_3\Phi_4\Phi_6B_{25} + \\
& \Phi_1\Phi_3\Phi_4\Phi_5B_{26} + \Phi_1\Phi_2\Phi_3\Phi_4B_{56} + \Phi_1\Phi_2\Phi_3\Phi_6B_{45} + \Phi_1\Phi_2\Phi_3\Phi_5B_{46} + \Phi_1\Phi_2\Phi_5\Phi_6B_{34} + \Phi_1\Phi_2B_{34}B_{56} + \\
& \Phi_1\Phi_2B_{35}B_{46} + \Phi_1\Phi_2B_{45}B_{36} + \Phi_1B_{23}\Phi_5B_{46} + \Phi_1B_{23}\Phi_4B_{56} + \Phi_1B_{23}B_{45}\Phi_6 + \Phi_1\Phi_3B_{24}B_{56} + \\
& \Phi_1\Phi_6B_{24}B_{35} + \Phi_1\Phi_5B_{24}B_{36} + \Phi_1\Phi_3B_{25}B_{46} + \Phi_1\Phi_6B_{34}B_{25} + \Phi_1\Phi_4B_{25}B_{36} + \Phi_1\Phi_3B_{45}B_{26} + \\
& \Phi_1\Phi_5B_{34}B_{26} + \Phi_1\Phi_4B_{35}B_{26} + \Phi_4\Phi_5B_{12}B_{36} + \Phi_3\Phi_4B_{12}B_{56} + \Phi_3\Phi_6B_{12}B_{45} + \Phi_3\Phi_5B_{12}B_{46} + \\
& \Phi_5\Phi_6B_{12}B_{34} + \Phi_4\Phi_6B_{12}B_{35} + \Phi_5\Phi_6B_{13}B_{24} + \Phi_4\Phi_6B_{13}B_{25} + \Phi_4\Phi_5B_{13}B_{26} + \Phi_2\Phi_4B_{13}B_{56} + \\
& \Phi_2\Phi_6B_{13}B_{45} + \Phi_2\Phi_5B_{13}B_{46} + \Phi_2\Phi_3B_{14}B_{56} + \Phi_2\Phi_6B_{14}B_{35} + \Phi_2\Phi_5B_{14}B_{36} + \Phi_5\Phi_6B_{23}B_{14} + \\
& \Phi_3\Phi_6B_{14}B_{25} + \Phi_3\Phi_5B_{14}B_{26} + \Phi_4\Phi_6B_{23}B_{15} + \Phi_3\Phi_6B_{24}B_{15} + \Phi_3\Phi_4B_{15}B_{26} + \Phi_2\Phi_3B_{15}B_{46} + \\
& \Phi_2\Phi_6B_{34}B_{15} + \Phi_{24}B_{15}B_{36} + \Phi_2\Phi_4B_{35}B_{16} + \Phi_4\Phi_5B_{23}B_{16} + \Phi_3\Phi_5B_{24}B_{16} + \Phi_3\Phi_4B_{25}B_{16} + \\
& \Phi_2\Phi_3B_{45}B_{16} + \Phi_2\Phi_5B_{34}B_{16}.
\end{aligned} \tag{18}$$

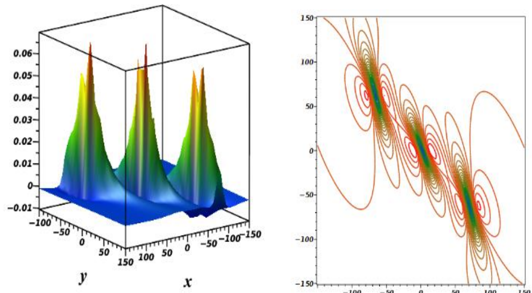

Fig. 4. Plots of 3-M-lump wave when $\boldsymbol{z = 2, t = 2, a_1 = 0.5, b_1 = 0.5, a_2 = \frac{1}{3}, b_2 = \frac{1}{3}, a_3 = \frac{1}{4}, b_3 = \frac{1}{4}, c_1 = 0.5, d_1 = 0.5, c_2 = \frac{1}{5}, d_2 = \frac{1}{5}, c_3 = \frac{1}{6}, d_3 = \frac{1}{6}, \beta = 2, \gamma = -1}$

DOI 10.2478/ama-2025-0026

We should know that $\Phi_p (p = 1, \ldots, 6)$, w_m, and B_{mn} are depicted in Eq. (13), Eq. (14) and Eq. (15), respectively. By introducing Eq. (18) into Eq. (5), a 3-M-lump solution is displayed in Fig. 4. It is important to understand that $l_1 = a_1 + b_1 i$, $l_2 = a_2 + b_2 i$, $l_3 = a_3 + b_3 i$, $l_4 = l_1^*$, $l_5 = l_2^*$, and $l_6 = l_3^*$.

3. COLLISION PHENOMENA

Through a long-wave approach and setting $k_m \to 0$, with $\frac{k_1}{k_2} = O(1)$, $e^{\lambda_m} = -1$ for $m = 1,2$, and $N = 3$, therefore f_3 reads

$$f_3 = \Phi_1\Phi_2 + B_{12} + \kappa_1 e^{\Psi_3}, \tag{19}$$

where

$$\kappa_1 = \Phi_1\Phi_2 + B_{12} + C_{23}\Phi_1 + C_{13}\Phi_2 + C_{13}C_{23}, \tag{20}$$

$$C_{mn} = -\frac{6k_n(1+l_m)(1+l_n)(2+l_m+l_n)}{3{k_n}^2(1+l_m)(1+l_n)^2-(l_m-l_n)^2\gamma}. \tag{21}$$

By combining Eq. (19) with Eq. (5), the outcome is a combination of a single-lump with a single-soliton solution (see Fig. 5).

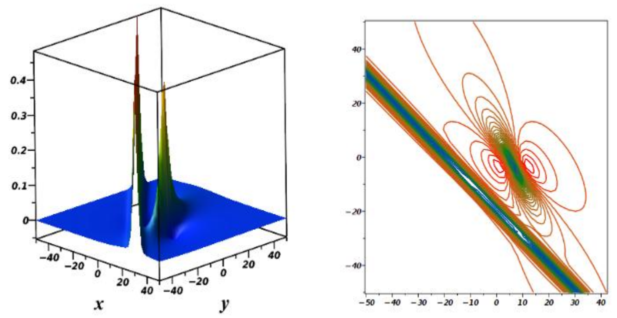

Fig. 5. Plots of M-lump with soliton solution when $\boldsymbol{z = 1, t = 2, a_1 = 0.5, b_1 = 0.5, a_2 = \frac{1}{3}, b_2 = \frac{1}{3}, k_3 = 1, l_3 = 1, j_3 = 2, \lambda_3 = 20, \beta = 2, \gamma = -1}$

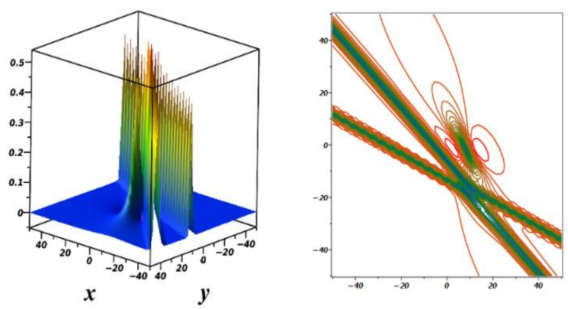

Fig. 6. Graphs of M-lump with a 2-soliton solution when $\boldsymbol{z = 1, t = 2, a_1 = 0.5, b_1 = 0.5, c_1 = \frac{1}{3}, d_1 = \frac{1}{3}, k_3 = 1, l_3 = 1, j_3 = 2, \lambda_3 = 10, k_4 = 1, l_4 = 2, j_4 = 3, \lambda_4 = 20, \beta = 1, \gamma = -5}$

Setting $N = 4$ in Eq. (7), and $k_m \to 0$, $\frac{k_1}{k_2} = O(1)$, and $e^{\lambda_m} = -1$ for $m = 1,2$, we set up

$$f_4 = \Phi_1\Phi_2 + B_{12} + \kappa_1 e^{\Psi_3} + \kappa_2 e^{\Psi_4} + A_{34} e^{\Psi_3+\Psi_4}(\kappa_1 + \kappa_2 - \Phi_1\Phi_2 - B_{12} + C_{13}C_{24} + C_{14}C_{23}), \tag{22}$$

where

$$\kappa_2 = \Phi_1\Phi_2 + B_{12} + C_{24}\Phi_1 + C_{14}\Phi_2 + C_{14}C_{24}. \tag{23}$$

Eq. (22) can be substituted into Eq. (5) to provide a result that combines the properties of a double-soliton solution and a single-M-lump solution (refer to Fig. 6).

If $N = 5$ and taking the limit $k_m \to 0$ and $e^{\lambda_m} = -1$ for $m = 1,2,3,4$, in Eq. (7), we get

$$f_5 = \Phi_1\Phi_2\Phi_3\Phi_4 + B_{34}\Phi_1\Phi_2 + B_{24}\Phi_1\Phi_3 + B_{23}\Phi_1\Phi_4 + B_{14}\Phi_2\Phi_3 + B_{13}\Phi_2\Phi_4 + B_{12}\Phi_3\Phi_4 + Qe^{\Psi_5} + B_{14}B_{23} + B_{13}B_{24} + B_{12}B_{34} \tag{24}$$

where

$$\begin{aligned} Q = {} & \Phi_1\Phi_2\Phi_3\Phi_4 + C_{45}\Phi_1\Phi_2\Phi_3 + C_{15}\Phi_2\Phi_3\Phi_4 \\ & + C_{25}\Phi_1\Phi_3\Phi_4 + C_{35}\Phi_1\Phi_2\Phi_4 \\ & + (B_{34} + C_{35}C_{45})\Phi_1\Phi_2 \\ & + (B_{24} + C_{25}C_{45})\Phi_1\Phi_3 \\ & + (B_{14} + C_{15}C_{45})\Phi_2\Phi_3 \\ & + (B_{23} + C_{25}C_{35})\Phi_1\Phi_4 \\ & + (B_{13} + C_{15}C_{35})\Phi_2\Phi_4 \\ & + (B_{12} + C_{15}C_{25})\Phi_3\Phi_4 \\ & + (B_{34}C_{25} + B_{24}C_{35} + B_{23}C_{45} \\ & + C_{25}C_{35}C_{45})\Phi_1 \\ & + (B_{34}C_{15} + B_{14}C_{35} + B_{13}C_{45} \\ & + C_{15}C_{35}C_{45})\Phi_2 \\ & + (B_{24}C_{15} + B_{14}C_{25} + B_{12}C_{45} \\ & + C_{15}C_{25}C_{45})\Phi_3 \\ & + (B_{23}C_{15} + B_{13}C_{25} + B_{12}C_{35} \\ & + C_{15}C_{25}C_{35})\Phi_4 + B_{14}B_{23} + B_{13}B_{24} \\ & + B_{12}B_{34} + B_{34}C_{15}C_{25} + B_{24}C_{15}C_{35} \\ & + B_{14}C_{25}C_{35} + B_{23}C_{15}C_{45} + B_{13}C_{25}C_{45} \\ & + B_{12}C_{35}C_{45} + C_{15}C_{25}C_{35}C_{45}. \end{aligned}$$

The outcome shown in Figure 7 is the observable feature, which is obtained by combining Eq. (24) and Eq. (5) to illustrate an interaction of a two-M-lump with a soliton solution. A complete list of all constants and functions can be found in this article.

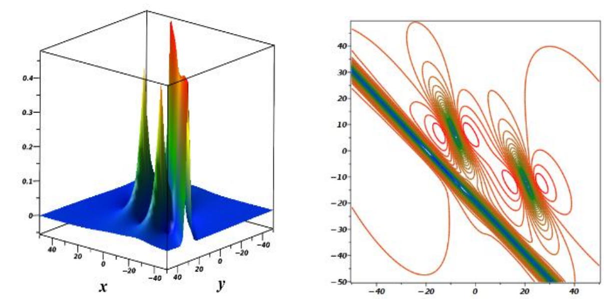

Fig. 7. Plots of 2-M-lump with soliton solution when $\boldsymbol{z = 1, t = 2, a_1 = 0.5, b_1 = 0.5, a_2 = \frac{1}{3}, b_2 = \frac{1}{3}, c_1 = \frac{1}{4}, d_1 = \frac{1}{4}, c_2 = \frac{1}{5}, d_2 = \frac{1}{5}, k_5 = 1, l_5 = 1, j_5 = 2, \lambda_5 = 20, \beta = 1, \gamma = -5}$

4. COMPLEX MULTI-SOLITON SOLUTIONS

Here, we explore the complexity of multi-solutions to the studied equation to explore new features of solutions.

DOI 10.2478/ama-2025-0026

4.1. The complex one-soliton wave

First, to construct the complex one-soliton wave, the assumption is

$$g_1=1+ie^{k_1\left(x+l_1y+j_1z-\left(1+{k_1}^2+j_1\beta+\frac{{l_1}^2\gamma}{1+l_1}\right)t\right)+\alpha_1}. \tag{25}$$

Substituting this assumption into Eq.(5), the result is

$$u=-\frac{2i{k_1}^2e^{\alpha_1+k_1\left(x+l_1y+j_1z-t\left(1+k_1^2+j_1\beta+\frac{{l_1}^2\gamma}{1+l_1}\right)\right)}}{\left(e^{\alpha_1+k_1\left(x+l_1y+j_1z-t\left(1+k_1^2+j_1\beta+\frac{{l_1}^2\gamma}{1+l_1}\right)\right)}-i\right)^2}. \tag{26}$$

This solution is shown graphically in Fig. (8).

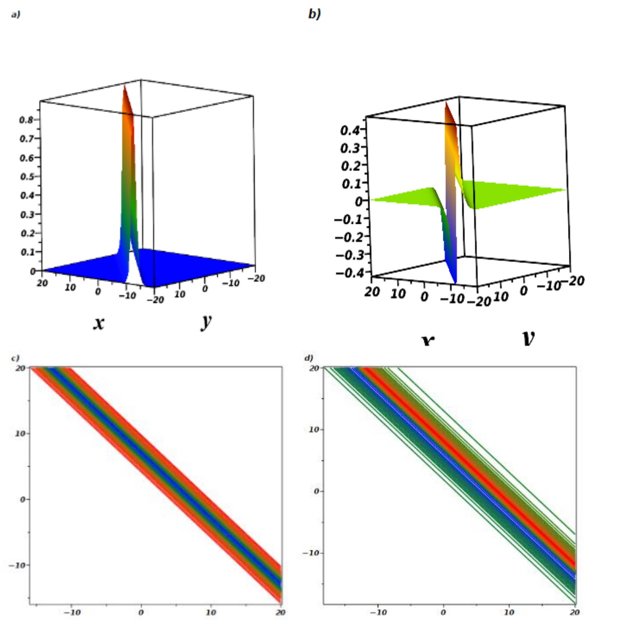

Fig. 8. Graphs of complex one-soliton wave are plotted for $z=1, t=2, k_1=1, l_1=1, j_1=2, \alpha_1=1, \beta=1, \gamma=2$: a) Real part, b) Imaginary part, c) Contour plot of real part, d) Contour plot of imaginary part

4.2. The complex two-soliton solution

Here, the objective is to drive a double-soliton solution, where the assumption is

$$g_2=1+ie^{\theta_1}+ie^{\theta_2}+S_{12}e^{\theta_1+\theta_2}. \tag{27}$$

Putting this equation into Eq. (5), the result yields

$$u=\frac{2\left(g_2\frac{\partial^2 g_2}{\partial x^2}-\frac{\partial g_2}{\partial x}^2\right)}{{g_2}^2}, \tag{28}$$

where

$\theta_1=k_1(x+l_1y+j_1z+\omega_1t)+\alpha_1, \theta_2=k_2(x+l_2y+j_2z+\omega_2t)+\alpha_2,\ \omega_1=-\left(1+{k_1}^2+j_1\beta+\frac{{l_1}^2\gamma}{1+l_1}\right), \quad \omega_2=-\left(1+{k_2}^2+j_2\beta+\frac{{l_2}^2\gamma}{1+l_2}\right)$

and

$$S_{12}=\frac{(l_1-l_2)^2\gamma-3(k_1-k_2)(1+l_1)(1+l_2)\big(k_1(1+l_1)-k_2(1+l_2)\big)}{3(k_1+k_2)(1+l_1)(1+l_2)(k_1+k_2+k_1l_1+k_2l_2)-(l_1-l_2)^2\gamma}.$$

This solution represents a complex two-soliton solution, and it is drawn in Fig. (9).

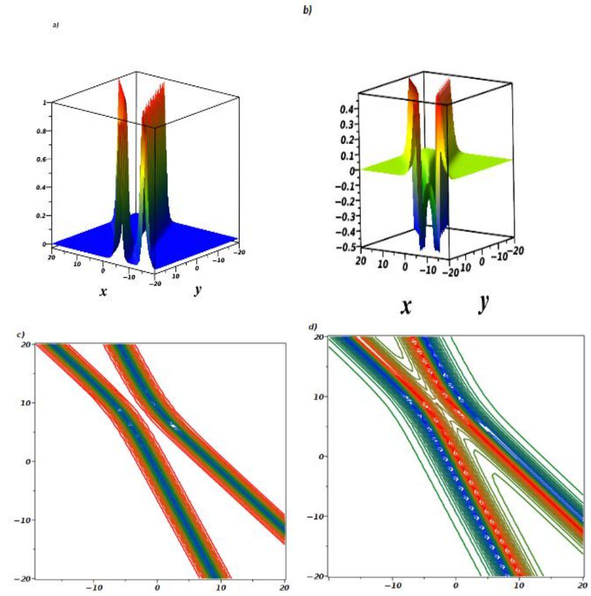

Fig. 9. Graphs of complex two-soliton wave are plotted for $z=1, t=2, k_1=1, k_2=1, l_1=1, l_2=0.5, j_1=0.5, j_2=0.5, \alpha_1=3, \alpha_2=6, \beta=1, \gamma=2$: a) Real part, b) Imaginary part, c) Contour plot of real part, d) Contour plot of imaginary part

4.3. The complex three-soliton solution

To report a three-soliton solution in complex form, let

$$g_3=1+ie^{\theta_1}+ie^{\theta_2}+ie^{\theta_3}+S_{12}e^{\varphi_1+\theta_2}+S_{13}e^{\theta_1+\theta_3}+S_{23}e^{\theta_2+\theta_3}+iS_{123}e^{\theta_1+\theta_2+\theta_3}. \tag{29}$$

Substituting this equation into Eq. (5), we have

$$u=\frac{2\left(g_3\frac{\partial^2 g_3}{\partial x^2}-\frac{\partial g_3}{\partial x}^2\right)}{{g_3}^2}. \tag{30}$$

The function θ_m is defined as

$$\theta_m=k_m(x+l_my+j_mz+\omega_mt)+\alpha_m, \tag{31}$$

with dispersion relation

$$\omega_m=-\left(1+{k_m}^2+j_m\beta+\frac{{l_m}^2\gamma}{1+l_m}\right), \tag{32}$$

where the constant $S_{123}=S_{12}S_{13}S_{23}$ $S_{123}=S_{12}S_{13}S_{23}$.

The constant S_{mn} is stated as

$$S_{mn}=\frac{Z_1}{Z_2}, \tag{33}$$

where

$Z_1=(l_m-l_n)^2\gamma-3(k_m-k_n)(1+l_m)(1+l_n)\big(k_m(1+l_m)-k_n(1+l_n)\big),$
$Z_2=3(k_m+k_n)(1+l_m)(1+l_n)(k_m+k_n+k_ml_m+$

DOI 10.2478/ama-2025-0026

$k_n l_n) - (l_m - l_n)^2\gamma.$

The result of this solution is presented in Fig. (10), which is a complex-three-soliton solution.

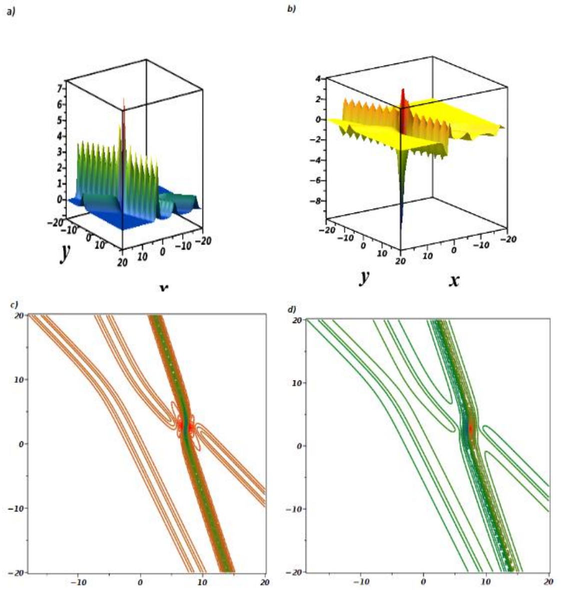

Fig. 10. Graphs of complex three-M-lump wave are plotted for $z = 1, t = 2, k_1 = 1, k_2 = 1, k_3 = 2, l_1 = 1, l_2 = 0.5, l_3 = \frac{1}{3}, j_1 = 0.5, j_2 = 0.5, j_3 = \frac{1}{3}, \alpha_1 = 3, \alpha_2 = 6, \alpha_3 = 9, \beta = 1, \gamma = 2$: a) Real part, b) Imaginary part, c) Contour plot of real part, d) Contour plot of imaginary part

4.4. The complex four-soliton solution

To report a four-soliton solution in complex form, let

$$g_4 = 1 + ie^{\varphi_1} + ie^{\varphi_2} + ie^{\varphi_3} + ie^{\varphi_4} + S_{12}e^{\varphi_1+\varphi_2} + S_{13}e^{\varphi_1+\varphi_3} + S_{14}e^{\varphi_1+\varphi_4} + S_{23}e^{\varphi_2+\varphi_3} + S_{24}e^{\varphi_2+\varphi_4} + S_{34}e^{\varphi_3+\varphi_4} + iS_{123}e^{\varphi_1+\varphi_2+\varphi_3} + iS_{124}e^{\varphi_1+\varphi_2+\varphi_4} + iS_{234}e^{\varphi_2+\varphi_3+\varphi_4} + S_{1234}e^{\varphi_1+\varphi_2+\varphi_3+\varphi_4} \quad (34)$$

where $S_{ijk} = S_{ij}S_{ik}S_{jk}$ and $S_{1234} = S_{123}S_{124}S_{234}$ are defined in Eq. (33). Substituting this equation into Eq. (5), we have

$$u = \frac{2\left(g_4\frac{\partial^2 g_4}{\partial x^2} - \frac{\partial g_4}{\partial x}^2\right)}{{g_4}^2}. \quad (35)$$

This equation represents a complex four-soliton solution (see Fig. (11)). The research paper contains all required constants and functions.

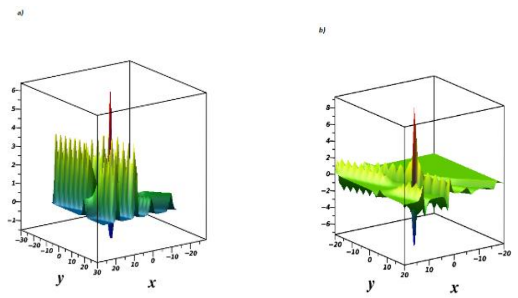

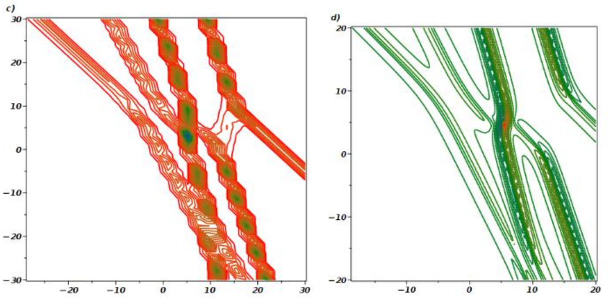

Fig. 11. Graphs of complex four-soliton wave are plotted for $z = 1, t = 2, k_1 = 1, k_2 = 1, k_3 = 2, k_4 = 2, l_1 = 1, l_2 = 0.5, l_3 = \frac{1}{3}, l_4 = \frac{1}{4}, j_1 = 0.5, j_2 = 0.5, j_3 = \frac{1}{3}, j_4 = \frac{1}{4}, \alpha_1 = 3, \alpha_2 = 6, \alpha_3 = 9, \alpha_4 = 12, \beta = 1, \gamma = 2$: a) Real part, b) Imaginary part, c) Contour plot of real part, d) Contour plot of imaginary part

5. RESULTS AND DISCUSSION

The gKdV equation has been investigated, and some novel solutions have been presented. A logarithmic variable transform is considered to transform the studied equation to the Hirota bilinear form. Via Hirota bilinear and long-wave methods, novel physical features to the considered equation are derived. The one-M-lump wave is shown in Fig. 1, and the motion of this wave, which moves on a straight line, is presented in Fig. 2. In Fig. 3 and Fig. 4, the double-, and triple-M-lump solutions have been drawn with the corresponding contour plots. Hybrid solutions are also derived. In Fig. 5 shows, mixed single soliton with a single M-lump wave, in Fig. 6 shows, mixed double soliton with a single M-lump wave, and Fig. 7 shows, mixed single soliton with a double M-lump wave with corresponding contour plots. Moreover, the complexiton soliton solutions are also constructed. In Fig. 8, the real and imaginary parts of a complex one-soliton solution are sketched. In Fig. 9, the real and imaginary parts of a complex two-soliton solution are drawn. The triple-soliton solution in complex form is derived in Fig. 10, and in Fig. 11, the behaviours of the four-soliton solution are presented.

6. CONCLUSION

We have considered the gKdV equation as a mathematical model of waves on shallow water surfaces. As far as macroscale processes and phenomena are concerned, KdV remains the most complete and arguably most useful model. First, the (3+1)-dimensional gKdV equation via variable transform is converted to the Hirota bilinear form. The M-lump wave solutions, namely one-lump, two-lump, and three-lump solutions, have been explored by applying the long-wave technique on the N-soliton solutions, which were constructed via the Hirota method. The interaction solutions via utilizing both Hirota bilinear and long-wave methods have been derived. These physical phenomena are one-soliton-lump, two-soliton-lump, and two-lump-soliton solutions. By virtue of the Hirota method, the N-complex-soliton solutions in complex form are constructed. The propagation characteristics of all gained solutions are shown graphically in 3D and contour plots. All phenomena presented in this work are verified by plugging them back into the studied equation. All presented physical phenomena are novel and have not been presented in the previously published study. In future work, these methods could be applied to more integrable NPDE and complex PDE to explore new features of solutions.

REFERENCES

1. Hirota R. The direct method in soliton theory. Cambridge University Press. 2004 (155).
2. Ismael HF, Sulaiman TA, Younas U, Nabi HR. On the autonomous multiple wave solutions and hybrid phenomena to a (3+ 1)-dimensional Boussinesq-type equation in fluid mediums. Chaos Solitons Fractals. 2024;187:115374.
3. Wazwaz A-M. The simplified Hirota's method for studying three extended higher-order KdV-type equations. Journal of Ocean Engineering and Science. 2016;1:181–5.
4. Ismael HF, Bulut H. Nonlinear dynamics of (2+ 1)-dimensional Bogoyavlenskii–Schieff equation arising in plasma physics. Math Methods Appl Sci 2021.
5. Zhao Z. Bäcklund transformations, rational solutions and soliton–cnoidal wave solutions of the modified Kadomtsev–Petviashvili equation. Appl Math Lett. 2019;89:103–10.
6. Hirota R. Soliton solutions to the BKP equations. I. The Pfaffian technique. J Physical Soc Japan 1989;58:2285–96.
7. Murad MAS, Ismael HF, Sulaiman TA. Resonant optical soliton solutions for time-fractional nonlinear Schrödinger equation in optical fibers. Journal of Nonlinear Optical Physics & Materials. 2024:2450024.
8. Peng W-Q, Tian S-F, Wang X-B, Zhang T-T, Fang Y. Riemann–Hilbert method and multi-soliton solutions for three-component coupled nonlinear Schrödinger equations. Journal of Geometry and Physics. 2019;146:103508.
9. Zhang Y, Cheng Y, He J. Riemann-Hilbert method and N-soliton for two-component Gerdjikov-Ivanov equation. Journal of Nonlinear Mathematical Physics. 2017;24:210–23.
10. Murad MAS, Ismael HF, Sulaiman TA. Various exact solutions to the time-fractional nonlinear Schrödinger equation via the new modified Sardar sub-equation method. Phys Scr. 2024;99:085252.
11. Peng W-Q, Chen Y. N-double poles solutions for nonlocal Hirota equation with nonzero boundary conditions using Riemann–Hilbert method and PINN algorithm. Physica D. 2022;435:133274.
12. Abdel-Gawad HI, Sulaiman TA, Ismael HF. Bright–dark envelope-optical solitons in space-time reverse generalized Fokas–Lenells equation: Modulated wave gain. Modern Physics Letters B. 2025;39:2450377.
13. Fan L, Bao T. The integrability and infinite conservation laws of a variable coefficient higher-order Schrödinger equation. Chinese Journal of Physics 2024.
14. Younas U, Muhammad J, Ismael HF, Murad MAS, Sulaiman TA. Optical fractional solitonic structures to decoupled nonlinear Schrödinger equation arising in dual-core optical fibers. Modern Physics Letters B. 2025;39:2450378.
15. Zhao X-H, Li S. Dark soliton solutions for a variable coefficient higher-order Schrödinger equation in the dispersion decreasing fibers. Appl Math Lett. 2022;132:108159.
16. Kaya D, El-Sayed SM. On a generalized fifth order KdV equations. Phys Lett A. 2003;310:44–51.
17. Butler S, Joshi N. An inverse scattering transform for the lattice potential KdV equation. Inverse Probl. 2010;26:115012.
18. Alharbi AR, Almatrafi MB. Exact solitary wave and numerical solutions for geophysical KdV equation. Journal of King Saud University-Science. 2022;34:102087.
19. Zhang D-J, Zhao S-L, Sun Y-Y, Zhou J. Solutions to the modified Korteweg–de Vries equation. Reviews in Mathematical Physics. 2014;26:1430006.
20. Salas AH, Gómez S CA. Application of the Cole-Hopf transformation for finding exact solutions to several forms of the seventh-order KdV equation. Math Probl Eng. 2010.
21. Ramirez J, Bruzón MS, Muriel C, Gandarias ML. The Schwarzian Korteweg–de Vries equation in (2+ 1) dimensions. J Phys A Math Gen. 2003;36:1467.
22. Lü X, Chen S-J. N-soliton solutions and associated integrability for a novel (2+ 1)-dimensional generalized KdV equation. Chaos Solitons Fractals. 2023;169:113291.
23. Ismaeel SME, Wazwaz A-M, El-Tantawy SA. New (3+ 1)-dimensional integrable generalized KdV equation: Painleve property, multiple soliton/shock solutions, and a class of lump solutions. Rom Rep Phys. 2024;76:102.
24. Novikov S, Manakov S V, Pitaevskii LP, Zakharov VE. Theory of solitons: the inverse scattering method. Springer Science & Business Media. 1984.
25. Satsuma J, Ablowitz MJ. Two-dimensional lumps in nonlinear dispersive systems. J Math Phys. 1979;20:1496–503.

Hajar Farhan Ismael: https://orcid.org/0000-0001-6189-9329